Advances of Optic Fiber Fabry-perot Interferometry Sensors

Yu Shen* and Zhi Zhou**

***Abstract**: Optic Fiber Fabry-Perot interferometry sensors (OF-FPI) provide the highest sensitivity among Optic Fiber sensors, and have been studied by many investigators. In order to measure various physical parameters with demanding precision, many designs have been proposed. In this review, the basic principles of OF-FPI sensors were demonstrated. Two beam optical interference equation has been adopted to modeling the sensor. Relationships of FP length and strain vs. the neighboring frequencies were demonstrated. Multiplexing technologies were also investigated. Several existing applications of OP-FPI sensors were also summarized including pressure, strain, temperature measurement. The state of the art designing of OP-FPI sensors provides with extreme accuracy and sensitivity. Trends in the development of this sensor technology and expected application areas are briefly outlined.*

***Keyword:** Optic Fiber, Fabry-Perot, sensor, interferometry*

INTRODUCTION

Every year, a significant amount of resources are allocated for the maintenance of civil, automobile and aerospace structures like bridges, airplane, buildings, etc. In recent years, as an alternative to manual surveying, embedded sensors for structural health monitoring has been demonstrated. Different types of sensors have been demonstrated for structural health monitoring including lead zirconate titanate (PZT) sensor, piezoelectric active sensors, electronic strain gauges and optical fiber based sensors. Amongst sensors applied in structural health monitoring, Optical fiber based sensors have gained wide interest in recent years.

Optic Fiber Fabry-perot interferometry sensor (OF-FPI) as one type of Fiber Optic Sensor has several advantages over conventional sensors: immunity to electromagnetic interference, ability to operate in harsh environments and potential for multiplexing. Its extremely sensitivity (Petuchowski, Giallorenzi et al. 1981) over other types of sensors has enabled the wide use for the demanding measurements of various physical quantities, such as temperature (Lee and Taylor 1991), strain (Valis, Hogg et al. 1990), pressure (Kao and Taylor 1996), refractive index (Xiao, Adnet et al. 2005), displacement (Wang, Zheng et al. 1998), vibration (Canuto 2006), etc. Due to its fabrication and operation differences, OF-FPI sensors are divided into two types: extrinsic FPI sensor(Furstenau, Schmidt et al. 1997) and intrinsic FPI sensor(Kao and Taylor 1996). The micro cavities of extrinsic FPI sensor are exposed into the environment enabling the measurement of refractive index in addition to other physical parameters. Whereas the intrinsic FPI sensor offers other benefits such as lower insertion loss and longer cavity since the light always transmits in the fiber core. This feature also enables the possibilities for large-scale multiplexing and quasi-distributed measurements.

Recently, OF-FPI sensors are applied to a variety of fields such as civil engineering (Claus, Gunther et al. 1992), materials science (Antunes, Travanca et al. 2012) , chemistry (Wang and Wang 2012), telecommunications, acoustics (Furstenau, Schmidt et al. 1997), biophysics (Zhang, Pathak et al. 2011), etc.

In this paper, the basic principles of OF-FPI sensors were demonstrated. Two beam optical interference equation has been adopted to modeling the sensor. Relationships of FP length and strain vs. the neighboring frequencies were demonstrated. Multiplexing technologies were also investigated. Several existing applications of OP-FPI sensors were also summarized including pressure, strain, temperature measurement. The state of the art designing of OP-FPI sensors provides with extreme accuracy and sensitivity. By utilizing the state of the art fabrication technologies a sensitivity of 5.35nm/kPa for pressure measurement, a resolution of 10 micro-strain

* *Master Candidate*
School of Civil Engineering
Dalian University of Technology, Dalian, China
Email: shenyu@mail.dlut.edu.cn

** *Corresponding author, Professor*
School of Civil Engineering
Dalian University of Technology, Dalian, China
Email: zhouzhi@dlut.edu.cn

within a $\pm 12\%$ dynamic range for strain measurement, a sensitivity of $143.5 \pm 1.0 nm/℃$ for temperature measurement can be achieved.

BASIC PRINCIPLES OF OF-FPI SENSOR

As shown in Fig.1, a typical experiment set up includes an input laser source, an optical spectrum analyzer (OSA), a coupler and the relevant computers for data processing. The laser source generate laser beam as input, a 3dB coupler was used to send the laser beam into the sensor and receive the reflected light. Then the OSA recorded the reflected light. The sensor head was subjected to the external environment to test the physical parameters.

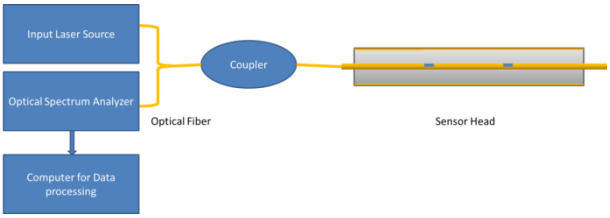

Fig.1 Experiment set ups for OF-FPI sensor

Light beam generated by the Laser Source propagates through the Optical Fiber, at a certain position a small proportion of light is reflected back due to the induced reflective index disturbance (Fig.2).

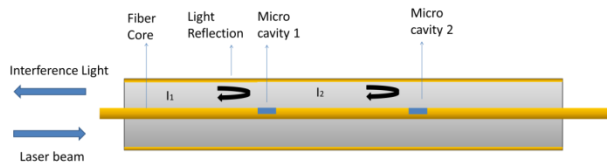

Fig.2 Basic principles of OF-FPI sensor

Two beams of reflected light can be modeled using the following equations:

$$\overrightarrow{E_1} = E_1 \cos(\omega t - \frac{2\pi r_1}{\lambda} + \varphi_0) \quad (1)$$

$$\overrightarrow{E_2} = E_1 \cos\left(\omega t - \frac{2\pi r_2}{\lambda} + \varphi_0\right) \quad (2)$$

In the equation, $\overrightarrow{E_1}$ and $\overrightarrow{E_2}$ are two light vectors. ω is the angular velocity, λ is the wavelength, r is the optical path length, φ_0 is the initial phase.

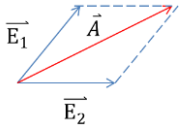

Fig.3 Vector Summation of reflected lights

The two beams of reflected light meet at the photo-detector ,in its essence as shown in the Fig.3, is the vector summation of two interference lights which can be described by the two-beam optical interference equation as follows:

$$A = \sqrt{E_1^2 + E_2^2 + 2E_1E_2\cos\Delta\psi} \quad (3)$$

$$\Delta\psi = 2\pi\frac{r_1 - r_2}{\lambda}$$

In the equation (X), A for the Amplitude of the interference light, $\Delta\psi$is the phase shift, r_1 and r_2 are the optical path length.

Assumes I_1 and I_2 are for the intensity of light, as we already know the intensity is two orders of Amplitude which are $I_1 = E_1^2, I_2 = E_2^2$, we have:

$$I = I_1 + I_2 + 2I_1I_2\cos\Delta\psi \quad (4)$$

Furthermore, if the loss of light travelling by pass the FP is little and neglected we have $I_1 = I_2$. If we sume $L = \frac{1}{2}(r_1 - r_2)$ as the length of the FP and 'n' for the refractive index, we can simplify the former equation.

$$I = 2I_1 + 2I_1^2\cos(4\pi\frac{nL}{\lambda}) \quad (5)$$

By applying the velocity of light equals frequency times wavelength $c = f\lambda$, we have another form of previous equation:

$$I = 2I_1 + 2I_1^2\cos(4\pi L\frac{nf}{c}) \quad (6)$$

The period of the interference light is $T = \frac{c}{2nL}$.

Here we have the most fundamental equations of FP sensor. In the field of civil engineering, the strain is of great concerns. Quite interesting, the length of the FP has a definite relation with the strain of FP. By looking back

to the equation (5) or (6), if the input frequency or wavelength of light varies, the intensity of the interference light varies as a sinusoidal function. For example, when L=0.2m, n=2 or L=0.21, n=2, scanning from 10MHz to 6GHz. The following graph is what we get at the OSA.

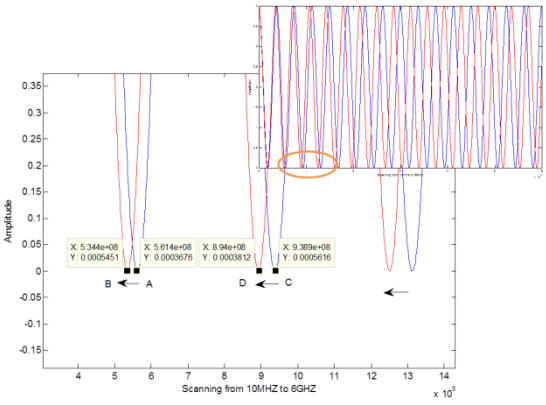

Fig.4 An example of interference spectrum.

In Fig.4, the blue curve shows the spectrum when L=20cm while the red one represent the spectrum when L=21cm. It is clear to tell, when L increases, the spectrum (A, C) move to the left.

From the Fig.4, the neighboring valley(A, C) of sinusoidal wave experiencing a phase shift of 2π. By referring to equation (6), we have:

$$4\pi L\frac{nf_2}{c} - 4\pi L\frac{nf_1}{c} = 2\pi$$

Simplifying the former equation we have:

$$L = \frac{C}{2(f_2 - f_1)n} \tag{7}$$

The Mth and the Nth valley have a phase shift of $2(M-N)\pi$, the equation (8) can be extended to:

$$L = \frac{C(M-N)}{2(f_M - f_N)n} \tag{8}$$

Equation (7) and (8) implies that we can get the FP length by measuring the neighboring frequencies of the valleys.

Next, another important equation shall be derived. In the Peak, we have $4\pi L_1\frac{nf_1}{c} = 2k\pi$, when deformation was induced the FP length will be changed to L_1 and the location of the peak-frequency will also be changed to f_2, at this stage we have $4\pi L_2\frac{nf_2}{c} = 2k\pi$, the right side is the same. We have $L_1f_1 = L_2f_2$, which is $L_2 = \frac{L_1f_1}{f_2}$, we already know $\varepsilon = \frac{L_2 - L_1}{L_1}$, then we get:

$$\varepsilon = \frac{f_1}{f_2} - 1 \tag{9}$$

So far we have all the equations of FP sensor. The FP length can be obtained by utilizing equation (7) (8). For example, in Fig.4 the frequencies of the 2nd and the 3nd valley are 564352176Hz and 938914457Hz. We have the FP length as 0.2002m where the true value is 0.2m. There is only 0.1% of error which dominates by the resolution of instrument. The strain of FP sensor after deformation can be obtained by utilizing equation (16). For example, in Fig.4 the frequencies in position A and B are 561355677.838919Hz and 534387193.596798Hz respectively. From equation (6) we have the strain of FP as 0.0505 where the true value is 0.05. Again the error is very limited, say only 1%.

MULTIPLEXING METHOD

&

SIGNAL RPOCESSING

Due to the FP sensor's low loss during reflecting, the light in the Optic Fiber can transmit in a long distance thus large reflections can be obtained. Quite like the traditional FBG sensor, the FP has great potentials to be multiplexed in a signal fiber. OF-FPI sensors may be multiplexed by time division, frequency division or WLI, which allows several sensors to be addressed with minimal cross-talk. The basic reflection principle of multi-FP sensors embedded in a single fiber shears with the previous single FP sensor. In order to get a general idea of multiplexing, in the first stage, we embed three FP sensors in one fiber and multiplexed them by utilizing frequency division multiplexing. This test is believed to give us some insights into the FP sensor multiplexing technology.

In this case, a single Optic Fiber with three cavities is presented in Fig.5. In each cavity, there is a slight disturbance of the reflective index thus a small proportion of light is reflected. Every two of those three cavities can form a FP sensor.

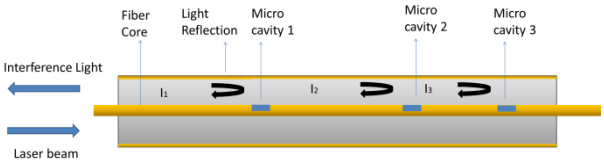

Fig.5 single Optic Fiber with 3 cavities

Assumes the first and second micro cavity forms the first FP sensor with a length of L1;Assumes the second and third micro cavity forms the second FP sensor with a length of L2;Assumes the first and third micro cavity forms the third FP sensor with a length of L3;Based on the equation (6) we have their interference equations:

$$I = 2I_1 + 2I_1^2\cos(4\pi L_1 \frac{nf}{c})$$

$$I = 2I_1 + 2I_1^2\cos(4\pi L_2 \frac{nf}{c})$$

$$I = 2I_1 + 2I_1^2\cos(4\pi L_3 \frac{nf}{c})$$

In the fiber end we receive a signal as follows:

$$I = 6I_1 + \sum_i^3 2I_1^2\cos(4\pi L_i \frac{nf}{c}) \qquad (10)$$

When L1=0.2;L2=0.5; c=3e8;n=2;I1=1; The following spectrum can be get at the Fiber end:

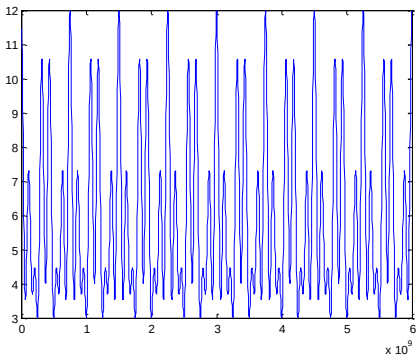

Fig.6 interference spectrum of three FP sensors in a single fiber

Apply Fast Fourier Transformation (FFT), a more clear graph can be obtained:

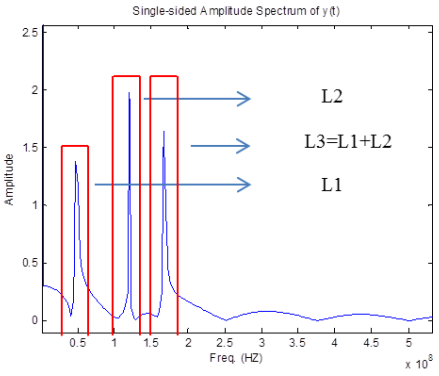

Fig.7 FFT of the interference spectrum

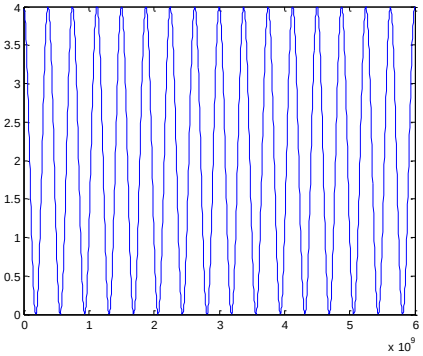

(a) FP1

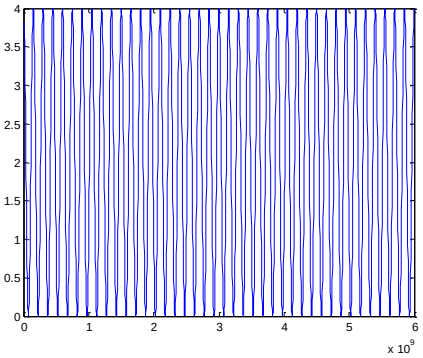

(b) FP2

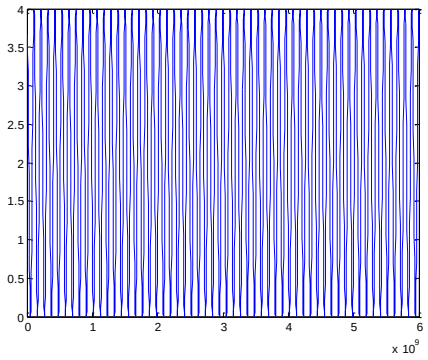

(C) FP3

Fig.8 The corresponding spectrum of each sensor

So far, each of the three FP sensors' information is obtained. Equations (7)-(9) can be then applied to get the data such as FP length, strain, etc.

When there are more than three cavities in the fiber, each of the cavity will reflect a small proportion of light, it is easy to derive the equation when multi-cavities are in a single fiber:

$$I = 6I_1 + \sum_i^N 2I_1^2 \cos(4\pi L_i \frac{nf}{c}) \quad (11)$$

The relationship of number of FP sensors and cavities are given below:

$$N = \frac{n(n-1)}{2} \quad (12)$$

When in practical use, the interferences between different FP sensors must be taken into consideration. FP cavity length should be chosen appropriately that their interference patterns were well separated when the OSA was scanned. If not, after applying FFT, the three FP sensors' interference spectrum can easily overlap on one another causing difficulties to signal processing. More sensors could be included utilizing frequency domain multiplexing, provided that the SNR is sufficient and Fabry-Perot sensors of appropriate length were provided. Modeling of a serially multiplexed arrangement suggested that operation with 5-10 sensors is possible (Kaddu, Collins et al. 1999). However, time domain multiplexing has a larger potential but require extra time to de-multiplex.

EXISTING APPLICATIONS OF OF-FPI SENSOR

Fabry-Perot interferometer sensors are often categorized as intrinsic Optic Fiber Fabry-Perot interferometer (OF-FPI) sensors in which the cavity is contained within the fiber and extrinsic Fabry-Perot interferometer sensors in which the cavity is external to the fiber. Based on different physical parameters to test, both intrinsic and extrinsic OP-FPI sensors are demonstrated among those years.

Pressure measurement

Pressure is force per unit area applied in a direction perpendicular to the surface of an object. Due to wide commercial usage and engineering concerns, pressure measurement technologies has been studied intensively over the years. Combined with the strength of high sensitivity and immunity from electric field, OP-FPI pressure sensors have drawn lots of attention.

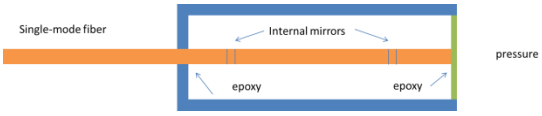

Fig.9 OF-FPI pressure sensor

A intrinsic pressure sensor design that combines the simplicity in calibration and signal processing of the OF-FPI sensor with the high sensitivity of a thin diaphragm is presented (Kao and Taylor 1996). The single-mode fiber containing the interferometer is bonded at one end to the diaphragm and is also attached under longitudinal tension beyond the interferometer to the sensor housing. The fiber is mounted under tension, so that pressure on the diaphragm causes a length change in the section of the fiber between the mirrors. One determines this length change by monitoring the reflectance of the interferometer. The predicted pressure sensitivity of the sensor is calculated from elasticity theory. This pressure sensor is reported to have a high sensitivity of 8.652×10^{-5} rad/Pa and a good Linearity over the range 0-100 Torr. This type of sensor is also suitable for operation with other signal processing and multiplexing schemes mentioned earlier. However, by utilizing this scheme might result in temperature induced error. Recently, a high performance multiplexed fiber-optic sensor consisted of diaphragm-based extrinsic Fabry-Perot interferometer and fiber Bragg grating is proposed (Wang, Jiang et al. 2012). The novel structure (Fig.10) fabricated with laser heating fusion technique possesses high sensi-

tivity with 5.35nm/kPa and exhibits ultra-low temperature dependence with 0.015nm/℃.

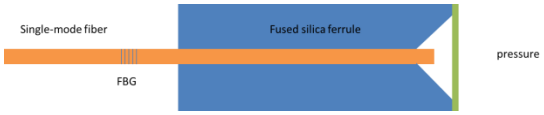

Fig.10 FBG OF-FPI multiplexed pressure sensor

The designed stainless epoxy-free packaging structure guarantees the FBG to be only sensitive to temperature. The temperature information is created to calibrate the pressure measurement error induced by the temperature dependence, realizing effectively temperature self-compensation of the multiplexed sensor.

Strain measurement

Strain is always of great concerns in civil engineering. Include several common advantages shared by Optic Fiber sensors, OF-FPI strain sensors have its' unique strength. A typical OP-FPI sensor is shown in Fig.2 and its basic principle has been investigated intensely in the first session. While in practical use, the extrinsic OP-FPI strain sensor offers the advantages over the intrinsic method are the avoidance of polarization problems and the detection of axial absolute strain components only (Claus, Gunther et al. 1992). A drawing detailing the construction of the extrinsic OP-FPI strain sensor is given in Fig.11

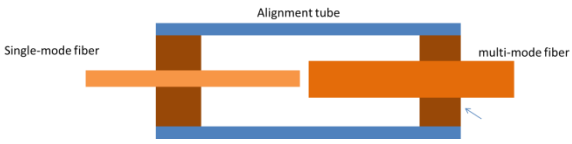

Fig.11 Schematic of the extrinsic OP-FPI strain sensor

In the schematic a single mode fiber is used as the input/output fiber, a multimode fiber is used purely as a reflector. The air gap between the single-mode fiber and multi-mode fiber forms acts as a low-finesse FP cavity. The far end of the multimode fiber is shattered so the reflections there do not add to the detector noise. The Fresnel reflection from the glass/air interface at the front of the air gap and the reflection from the air/glass interface at the far end of the air gap interfere in the input/output fiber. The two fibers are allowed to move in the silica tube and changes in the length cause changes in the phase difference between the reference reflection and the sensing reflection. The Alignment tube can be attached to the surface or bonded within the structure for strain measurement. Materials with low thermal expansion ratios would be preferred for the alignment tube. The crosstalk induced by temperature elevation could be reduced significantly. This schematic may also be used as displacement sensor by attaching one fiber to a stationary block and the second fiber to a moving block. This device is reported to be valid over a -200-900℃ temperature range.

Under extreme loads, such as earthquakes and landslides, structures are often experience excessive deformation and subjected to a strain in the order of 10 000 to 100 000 micro strain. Therefore, large-strain capable sensors are desired in the field of Structure Health Monitoring. Recently, a large strain enabled extrinsic OF-FPI sensor with high resolution is proposed by Ying Huang, Tao Wei, Zhi Zhou of Missouri University of Science and Technology (Huang, Wei et al. 2010).

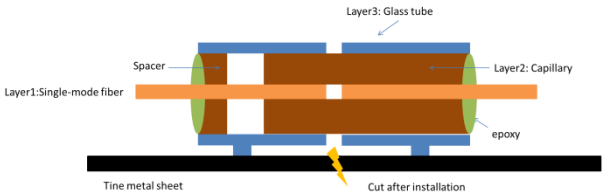

Fig.12 Schematic of large strain capable sensor

The sensor is formed by two perpendicularly cleaved end faces of a single-mode optical fiber (Fig.12). The left side of the fiber serves as a lead-in fiber, and the other side serves as a low reflective mirror. To ensure the both sides keeps in the same axis and remain intact during large strain, a three-layer structure is used to package the strain sensor, including the core, intermediate and outmost layers. Layer 1 is an optical glass fiber. The Layer 2 is a capillary glass tube designed to guide the cleaved fiber to ensure that its two end faces can move in parallel. Layer 3 is a glass tube designed to enhance the overall stability of the packaged sensor. At both end the layers are bonded together with epoxy. The real trick is all the layers are bonded together on the right side. While on the right side the fiber is bonded to the third layer through an inserted spacer to allow for free movement of the fiber end faces within the capillary tube. The tine metal sheet is used to bolt the sensor to a steel substructure during applications. After installed and before operating the thin metal sheet is separated as indicated in Fig.12 It is reported the sensor has a strain resolution of 10 micro-strain within a $\pm$12% dynamic range.

Temperature measurement

OF-FPI sensors for temperature measurement have drawn lots of attention over the years because of its low fabrication costs and excellent performance under extreme temperature. When applied in temperature measurement, intrinsic OF-FPI sensors are more preferred. They have smaller cross-sectional areas which allow their consolidation into structures with minimum intrusion. While the extrinsic OF-FPI sensors are easier to fabricate but the reflectance of the air/fiber interfaces cannot be altered. Quite like Fig.2 the internal mirrors or the FP cavities can be reflective splices between two identical fibers, two different fibers, or two fiber Bragg gratings. For example, a FP sensor formed with two reflective splices along a SMF, where the two end faces of the fiber to be spliced onto the other fiber are coated with TiO_2 films (Kaddu, Collins et al. 1999), has been demonstrated for temperature measurement up to 1050℃. An in fiber FP cavity can also be formed by micro-machining a fiber with laser pluses (Wei, Han et al. 2008). Such a rigid structure can withstand a temperature up to 800℃.

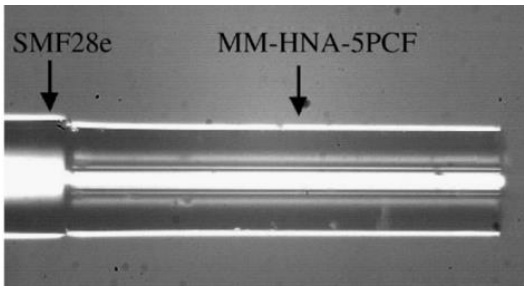

Fig.13 Micro images of fabricated sensor

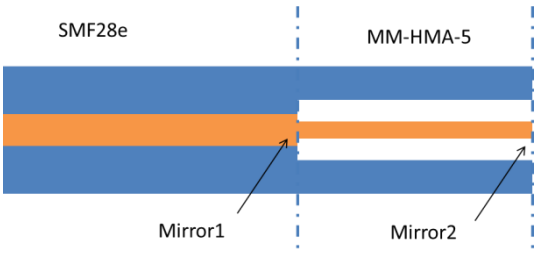

Fig.14 Schematic of sensor

Recently, a novel OF-FPI tip sensor capable for temperature up to 1200℃ was reported (Zhu, Ke et al. 2010). The FP cavity was formed by splicing a short length of a special photonic crystal fiber (PCF) (Crystal Fiber, MM-HNA-5) to a SMF (Corning, SMF28e). The fabricated sensors show good linearity and exceptionally high sensitivity over the temperature range from -20℃ to +1200℃. Two distinct advantages are noticeable: (1) the higher reflection from the splice between the lead fiber and the PCF (due to the large air holes in the PCF) results in better fringe visibility and hence a higher signal-to-noise ratio; (2) the all-silica PCF cavity can measure higher temperature because of its higher glass transformation temperature. The fabricated sensor is shown in Fig.13 and the schematic of sensor is shown is Fig.14. The measured temperature sensitivities for the sensors with $L_0 = 575\mu m$ and $L_0 = 4785\mu m$ were $17.2 \pm 1.0\text{nm}/℃$ and $143.5 \pm 1.0\text{nm}/℃$ respectively.

SUMMARY AND CONCLUSION

Among Optic Fiber sensors, Fabry-Perot Interferometry Sensors provide the greatest flexibility and highest sensitivity for measuring very small physical parameters change. As a result of years of research, a well-developed technology in the area of OF-FPI sensors has evolved. Many applications have been found in the measurement of pressure, strain, temperature as mentioned above but not limited. The current sensitivity for pressure measurement are 5.35nm/kPa exhibits ultra-low temperature dependence with 0.015nm/℃. For strain measurement, a resolution of 10 micro-strain within a $\pm$12% dynamic range can be achieved. For temperature measurement, a sensitivity of $143.5 \pm 1.0\text{nm}/℃$ can be achieved. When it comes to the measurement of reflective index and bio-sensing, there has been an increasing application of OF-FPI sensors.

Substantial progress has been realized and has been manifested in the form of new classes of sensors with unparalleled sensitivity, geometric versatility and integrability. Efforts are presently under way to take the initially developed sensors tested in controlled environments and to incorporate them in full field demonstrations. Although there existing some difficulties in multiplex quantities of OF-FPI sensors, more and more researchers are focusing on the multiplexing technology to achieve quasi-distributed sensing. There are also potentials for OF-FPI sensors to integrate with the conventional sensors such as FBG to achieve more demand requirements. What's more, multi physical parameters measurements by splicing more than one OF-FPI sensors are emerging recently (Wang and Wang 2012).

In summary, OF-FPI sensor technology has progressed rapidly during the past decades and the technical advantages are well documented and reviewed in this paper. Unique properties and outstanding sensitivity for several of the sensors were demonstrated. We can conclude that OF-FPI sensors will impact existing sensor markets in a significant fashion and that several sensing functions

which were previously difficult to perform now become tractable and amenable to solution. During the next few years the viability of this technology will be established and substantial growth is expected.

REFERENCES

[1] Antunes, P., et al. (2012). "Dynamic Structural Health Monitoring of Slender Structures Using Optical Sensors." Sensors 12(5): 6629-6644.

[2] Canuto, E. (2006). "Active vibration suppression in a suspended Fabry-Perot cavity." Isa Transactions 45(3): 329-346.

[3] Claus, R. O., et al. (1992). "Extrinsic Fabry-Perot sensor for strain and crack opening displacement measurements from -200 to 900degC." Smart Materials and Structures 1(3): 237-242.

[4] Furstenau, N., et al. (1997). "Extrinsic Fabry-Perot interferometer vibration and acoustic sensor systems for airport ground traffic monitoring." Iee Proceedings-Optoelectronics 144(3): 134-144.

[5] Huang, Y., et al. (2010). "An extrinsic Fabry-Perot interferometer-based large strain sensor with high resolution." Measurement Science & Technology 21(10).

[6] Kaddu, S. C., et al. (1999). "Multiplexed intrinsic optical fibre Fabry-Perot temperature and strain sensors addressed using white-light interferometry." Measurement Science & Technology 10(5): 416-420.

[7] Kao, T. W. and H. F. Taylor (1996). "High-sensitivity intrinsic fiber-optic Fabry-Perot pressure sensor." Optics Letters 21(8): 615-617.

[8] Lee, C. E. and H. F. Taylor (1991). "FIBEROPTIC FABRY-PEROT TEMPERATURE SENSOR USING A LOW-COHERENCE LIGHT-SOURCE." Journal of Lightwave Technology 9(1): 129-134.

[9] Petuchowski, S. J., et al. (1981). "A SENSITIVE FIBEROPTIC FABRY-PEROT-INTERFEROMETER." Ieee Journal of Quantum Electronics 17(11): 2168-2170.

[10] Valis, T., et al. (1990). "FIBER OPTIC FABRY-PEROT STRAIN-GAUGE." IEEE Photonics Technology Letters 2(3): 227-228.

[11] Wang, T. T. and M. Wang (2012). "Fabry-Perot Fiber Sensor for Simultaneous Measurement of Refractive Index and Temperature Based on an In-Fiber Ellipsoidal Cavity." IEEE Photonics Technology Letters 24(19): 1733-1736.

[12] Wang, T. Y., et al. (1998). "A high precision displacement sensor using a low-finesse fiber-optic Fabry-Perot interferometer." Sensors and Actuators a-Physical 69(2): 134-138.

[13] Wang, W. H., et al. (2012). "Temperature self-compensation fiber-optic pressure sensor based on fiber Bragg grating and Fabry-Perot interference multiplexing." Optics Communications 285(16): 3466-3470.

[14] Wei, T., et al. (2008). "Temperature-insensitive miniaturized fiber inline Fabry-Perot interferometer for highly sensitive refractive index measurement." Optics Express 16(8): 5764-5769.

[15] Xiao, G. Z., et al. (2005). "Monitoring changes in the refractive index of gases by means of a fiber optic Fabry-Perot interferometer sensor." Sensors and Actuators a-Physical 118(2): 177-182.

[16] Zhang, T. H., et al. (2011). "A polymer nanostructured Fabry-Perot interferometer based biosensor." Biosensors & Bioelectronics 30(1): 128-132.

[17] Zhu, T., et al. (2010). "Fabry-Perot optical fiber tip sensor for high temperature measurement." Optics Communications 283(19): 3683-3685.